Sensors and Materials, Vol. 38, No. 7 (2026) 3747–3758
MYU Tokyo

S & M 4533

Suitability of Satellite Images with Different Resolutions for Information Extraction—An Example of Mango Groves

Yin Siyang,[1,2] Ren Chuanshuai,[3] Zhang Yi,[1,2*] Zhuang Yuan,[1,2] and Wu Shuang[1,2]

[1]Beijing Institute of Surveying and Mapping, Beijing 100038, China
[2]Beijing Key Laboratory of Urban Spatial Intelligent Sensing and Digital Governance, Beijing 100038, China
[3]Key Laboratory of Digital Earth Science, Aerospace Information Research Institute, Chinese Academy of Sciences, Beijing 100094, China

(Received October 17, 2024; accepted June 3, 2026)

Keywords: satellite images, different resolutions, mango groves, information extraction

The mango planting industry in China has been developing rapidly, but the spatial distribution information of mango groves has traditionally relied on slow and inefficient manual surveys. Therefore, it is urgent to study the remote sensing extraction method for mango groves. While numerous studies have focused on forest or agricultural information extraction using remote sensing techniques, studies specifically targeting mango grove extraction are scarce. In this study, we analyzed the suitability of remote sensing images with varying resolutions for the extraction of mango groves. Considering the spacing characteristics of mango groves, we generated remote sensing images with resolutions of 2, 4, and 8 m by downsampling 1 m GaoFen-2 data. The support vector machine method was employed to extract mango groves from these images with different resolutions. The results indicated that the highest accuracy was achieved using remote sensing images with a resolution of 2 m, whereas the extraction accuracy of images with a resolution of 1 m was slightly lower. In contrast, the extraction accuracy obtained from remote sensing images with resolutions of 4 and 8 m was low, as it was prone to misclassify mango groves with cultivated land at these resolutions. Therefore, satellite images with a resolution of 2 m are recommended for the extraction of mango groves, as they offer an optimal balance between classification accuracy and processing efficiency.

1. Introduction

Mango is one of the most popular tropical fruits in the world, renowned for its delicate taste, delightful aroma, and rich nutritional value. Mangoes are grown in over 100 countries worldwide, with a total fruit production exceeding 59 million metric tons. As the mango industry experiences rapid expansion, the costs associated with manual management are on the rise. Consequently, the adoption of remote sensing technology in mango grove management has emerged as an inevitable trend in the evolution of mango cultivation.(1) Remote sensing technology, with its ability for a synoptic view, provides a better alternative for agricultural

*Corresponding author: e-mail: 847979730@qq.com
https://doi.org/10.18494/SAM5399

ISSN 0914-4935 © MYU K.K.

management than traditional methods.[2] In recent decades, the spatial and temporal resolutions of remote sensing data have undergone a remarkable enhancement, enabling the prompt, precise, and exhaustive extraction of mango information, thereby facilitating better understanding and management of the spatial distribution of mango resources.[3]

The spatial resolution of remote sensing imagery describes the level of spatial detail of surface features and reflects the capability of images to separate target features from the background environment.[4–6] When using remote sensing imagery for land use/cover classification, fine spatial resolution can reduce the number of mixed pixels, so the images with higher resolution have the potential to improve the classification accuracy.[7–9] However, remote sensing imagery with excessively high spatial resolution may increase the spectral variability of the same categories, potentially reducing classification accuracy.[10–12] Mango groves, being planted in artificial rows, will form different mixed pixels with their surrounding soil background on the remote sensing imagery of varying spatial resolutions, leading to differences in spectral characteristics across remote sensing images with different spatial resolutions. Existing studies indicate that resolutions finer than 10 m can significantly compromise the accuracy of agricultural land-use classification.[13] In agricultural and orchard studies, resolutions of 1, 2, 4, and 8 m are commonly employed to analyze the extraction of remote sensing imagery with varying spatial resolutions.[14,15] In this study, we resampled GF-2 imagery to obtain images with four different spatial resolutions, comparatively analyzed the effects of images with different spatial resolutions on the extraction of mango groves, and ultimately determined the optimal spatial resolution of remote sensing images for the extraction of mango groves.

2. Data, Materials, and Methods

2.1 Study area

The study area is located in Sanya City, Hainan Province, China. Sanya City is located in the southernmost part of Hainan Province (18°09’34”–18°37’27”N, 108°56’30”–109°48’28”E). The district covers an area of 1920 km^2, with complex terrain, mainly including mountains, hills, and plains. Sanya City has the tropical marine monsoon climate, with an annual average temperature of 25.7 ºC. The highest temperature is in June with an average of 28.7 ºC, and the lowest temperature is in January, with an average of 21.4 ºC. The average annual rainfall is 1930.7 mm. Land use types mainly include cultivated lands, orchards, forests, urban construction lands, transportation lands, and lands for water conservancy facilities (Fig. 1). Orchards include mango

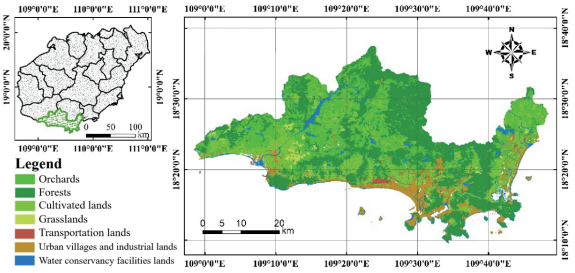

Fig. 1. (Color online) Land use type map of Sanya City.

groves and banana orchards. According to the Hainan Statistical Yearbook, the total area of garden fruit cultivation in Sanya in 2015 was 212 km^2, including 188 km^2 of mango groves and 16 km^2 of banana orchards. In recent decades, the mango industry in Sanya City has developed rapidly and the mango planting area has increased yearly. In 1991, the area of mango groves in Sanya was 8 km^2, and in 2023, the mango planting area exceeded 200 km^2, becoming the main tropical fruit species in Sanya.

2.2 Data and materials

2.2.1 Remote sensing data

In this study, the data of the Gaofen-2 (GF-2) satellite was selected as the data source of remote sensing images. The GF-2 satellite is the first batch of important projects to be developed in China's "Gaofen Special Project". To achieve the goal of "all-day and all-weather earth observation combined with medium- and low-resolution satellites", the GF-2 satellite is configured with four multispectral (MS) segments and one full panchromatic (PAN) segment, which can meet the requirements of remote sensing images for the extraction of mango groves. The image was clear and cloudless with good quality, which was conducive to the extraction of mango groves in the study area. Remote sensing images were preprocessed by radiometric calibration, atmospheric correction, and orthographic correction. The main parameters of the satellite and sensor are shown in Table 1.

2.2.2 Field data

To understand the spatial distribution of mango groves, field observations were conducted in the study area during the month of remote sensing image acquisition, and observations from a total of 181 typical sampling plots were collected. The distribution of sampling plots is shown in Fig. 2. According to the location of sampling plots and the corresponding field photos, the remote sensing image was connected with the field sampling plots, and the collection of features of remote sensing images (Table 2) was established to improve basic reference for the understanding of the surface features on remote sensing images.

Table 1
Orbit and attitude control parameters of GF-2 satellite.

Parameter	Index	Parameters	Index
Orbit type	Sun-synchronous return orbit	Wavelength range	PAN: 0.45–0.90 μm MS: 0.45–0.52 μm 0.52–0.59 μm 0.63–0.69 μm 0.77–0.89 μm
Orbital altitude	631 km		
Inclination angle	97.9080°		
Landing point descending node local time	10:30 AM		
Lateral sway capability	±35°, with a maneuver time of ≤180 seconds to achieve a 35° sway		
Spatial resolution	PAN: 1 m; MS: 4 m	Revisit period	5 days
Width	45 km (Dual-camera)	Coverage period	69 days

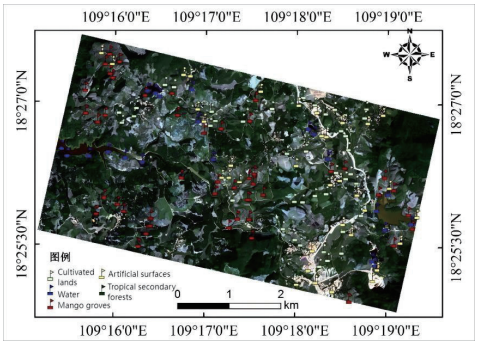

Fig. 2. (Color online) Distribution of ground survey samples in the study area.

Table 2
(Color online) Collection of features of remote sensing images in the study area.

Categories	Imaging features	Field photographs
Mango groves	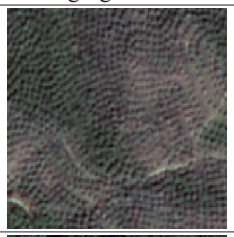	
Tropical secondary forests		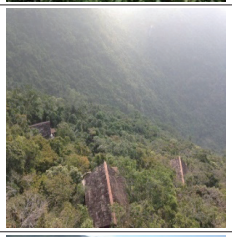
Cultivated lands	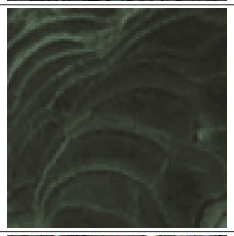	
Artificial surfaces		
Water body	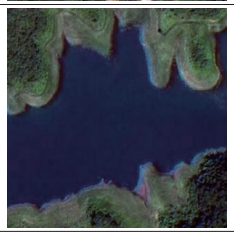	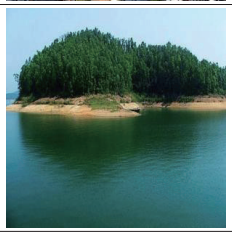

2.3 Methods

2.3.1 NND method

The nearest-neighbor diffusion (NND) method is a new method proposed by the Rochester Institute of Technology. In this method, the relationship between the gray values of adjacent pixels of MS images is fully taken into account in image fusion, so that the texture, color, and spectral information of the fused image can be well preserved.[16,17] The fusion image obtained by this method not only has the characteristics of high spatial and spectral resolutions, but also can reveal the internal information of multiband images more accurately and distinguish different ground object types according to color.[18] In this study, the 1 m panchromatic band and 4 m MS bands of the original GF-2 image were fused using the NND fusion algorithm. This process generated a four-band output image comprising red, green, blue, and NIR bands at a spatial resolution of 1 m.

2.3.2 SVM method

The support vector machine (SVM) method is based on the principle of minimum structural risk and the Vapnik–Chervonenkis (VC) dimension theory of statistical theory, and seeks the best classification method between the complexity and learning ability of the model according to the sample information provided. It has many advantages in solving nonlinear, small-sample, and high-dimensional pattern recognition, and has been widely used in many fields.[19–21] The SVM method was originally developed to solve binary classification problems. Its basic idea is as follows: SVM aims to find an optimal hyperplane for classification, such that the margin between the two classes of adjacent sample points is maximized.[22] The points on the maximized edge are called support vectors, and the middle section of the edge is the optimal classification hyperplane. To reduce the impact of points misassigned by edges on classification, the weight of misassigned points is reduced. When the data are linearly indivisible, the kernel function can be used to map the data points to a high-dimensional space to make them linearly separable. In recent years, many scholars have proved that the SVM classification algorithm has its unique advantages in the remote sensing extraction of vegetation. For example, Bazi and Melgani[23] compared the extraction accuracy of vegetation in the study area under SVM classification and neural network classification, and concluded that SVM classification was superior to neural network classification. Wang *et al.*[24] improved the accuracy of image classification by optimizing the parameters of the SVM algorithm, and proved that the optimized SVM algorithm achieved higher classification accuracy than other classification methods. Deng *et al.*[25] used SVM to extract urban green space in the study area, proving the applicability of SVM classification in the remote sensing extraction of urban green space information. Pouteau *et al.*[26] used SVM and random forest to extract native vegetation and rare vegetation, respectively, in southern France, and finally proved that SVM classification was more applicable in the extraction of rare vegetation.

On the basis of the information of 181 sample points investigated on the ground, the training samples were selected on the corresponding remote sensing images, and the spectral bands of the four types of spatial resolution remote sensing images resampled after fusion were classified by SVM classification. Using spectral information from the blue, green, red, and NIR bands, we developed an SVM classification model to generate the land cover classification results of the study area based on field data. The classified land cover types include mango groves, tropical secondary forests, cultivated lands, artificial surfaces, and water bodies. Moreover, the spatial resolution of the image with the best extraction effect was finally determined through the comparative analysis of the remote sensing extraction accuracy of mango groves.

3. Results

3.1 Fusion of remote sensing images

To study the effect of spectral images with different spatial resolutions on the information extraction of mango groves, the 1 m panchromatic and 4 m MS bands of the original GF-2 image were fused using the NDD fusion algorithm. Taking into account the characteristics of the line spacing of mango grove planting and the resolution settings of GF-1 and GF-2 satellites in China, on the basis of fusing the original GF-2 image into 1-m-resolution data, we used the mean resampling method to resample the 1 m fusion image and obtained resampling data with resolutions of 2, 4, and 8 m, respectively. Finally, four resolution image data are formed, namely, 1, 2, 4, and 8 m resolution data. The data of different resolutions are shown in Fig. 3.

3.2 Extraction of mango groves

On the basis of field sampling data, representative objects are selected as training samples, and SVM is used to classify four spatial resolution remote sensing images. The verification samples were selected for each object type at each resolution, and the error matrix was constructed to obtain the producer's accuracy (PA), user's accuracy (UA), omission error, and commission error after classification. The optimal spatial resolution of mango grove remote sensing extraction was presented by comparing and analyzing the precision.

The PA and UA of mango groves under the four spatial resolutions were compared and analyzed (Table 3). After resampling the 1-m-resolution image to 2 m, both the PA and UA of mango groves improved, in which the PA and UA increased by 2 and 1.6%, respectively. At a spatial resolution of 4 m, the PA of mango groves further improved, but the UA decreased considerably. In general, the extraction accuracy of mango grove remote sensing was lower at a resolution of 4 m than at a resolution of 2 m. At a resolution of 8 m, the UA of mango groves decreased to 58.25%, and the mixing between mango groves and other land species became more severe. In summary, when only the spectral information of the image is used, the mango grove extraction accuracy is higher with the image resolution of 2 m.

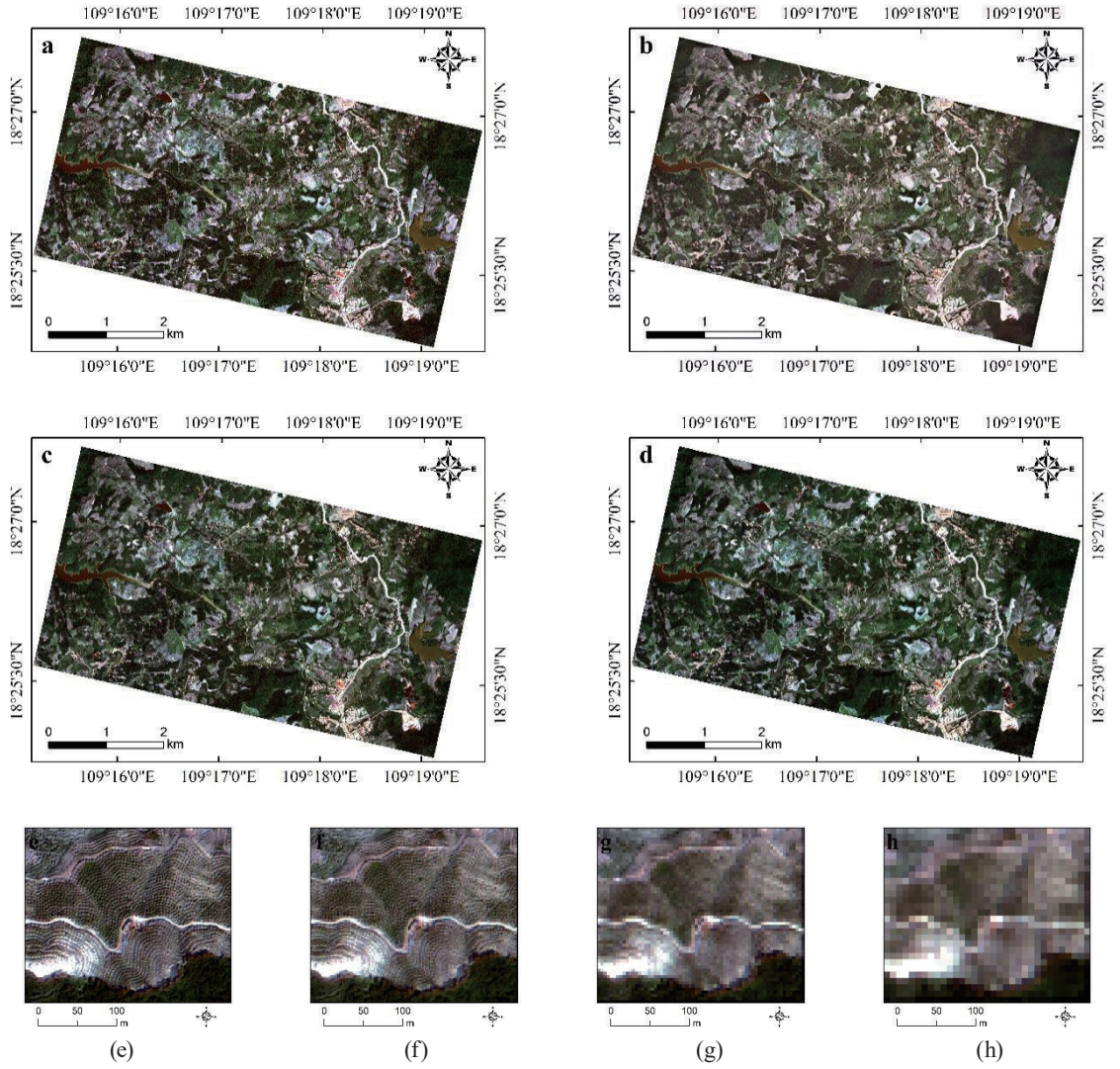

Fig. 3. (Color online) Images of mango groves in the study area and local areas under different resolutions: (a) 1-m-resolution image of the study area, (b) 2-m-resolution image of the study area, (c) 4-m-resolution image of the study area, (d) 8-m-resolution image of the study area, (e) local 1-m-resolution image of mango groves, (f) 2-m-resolution image of mango groves in local area, (g) 4-m-resolution image of mango groves in local area, and (h) 8-m-resolution image of mango groves in local area.

Table 3
Extraction accuracy of mango groves under four resolutions.

Spatial resolution	1 m	2 m	4 m	8 m
PA (%)	66.67	68.67	71.08	72.29
UA (%)	84.85	86.43	72.84	58.25
Omission error (%)	33.33	31.33	28.92	27.71
Commission error (%)	15.15	13.57	27.16	41.75

To further analyze the main factors of mango grove leakage under four spatial resolutions, the confusion matrix of the classification accuracy of the study area under four resolutions was constructed, and the results are shown in Tables 4 to 7.

From Tables 4 to 7, it can be found that under the four resolutions, cultivated lands are the main type of land that reduces the extraction accuracy of mango groves. Under the resolution of 1 m, 29.76% of mango groves were misclassified as cultivated lands and 11.67% of cultivated lands were misclassified as mango groves. At the resolution of 2 m, 27.71% of mango groves were divided into cultivated lands and 13.33% of cultivated lands were divided into mango groves. At the resolution of 4 m, 26.51% of mango groves were divided into cultivated lands, and

Table 4
Error matrix of 1-m-resolution image classification (%).

		Reference Image				
		Mango groves	Tropical secondary forests	Cultivated lands	Artificial surfaces	Water body
Evaluated Image	Mango groves	66.67	0.00	11.67	5.36	0.00
	Tropical secondary forests	2.38	40.98	11.67	0.00	0.00
	Cultivated lands	29.76	59.02	73.33	0.00	0.00
	Artificial surfaces	0.00	0.00	1.67	92.86	0.00
	Water body	0.00	0.00	0.00	1.79	100.00
	Others	1.19	0.00	1.67	0.00	0.00
	Total	100.00	100.00	100.00	100.00	100.00

Table 5
Error matrix of 2-m-resolution image classification (%).

		Reference Image				
		Mango groves	Tropical secondary forests	Cultivated lands	Artificial surfaces	Water body
Evaluated Image	Mango groves	68.67	0.00	13.33	8.93	0.00
	Tropical secondary forests	3.62	60.66	15.00	0.00	0.00
	Cultivated lands	27.71	39.34	70.00	0.00	0.00
	Artificial surfaces	0.00	0.00	1.67	89.29	0.00
	Water body	0.00	0.00	0.00	1.79	100.00
	Others	0.00	0.00	0.00	0.00	0.00
	Total	100.00	100.00	100.00	100.00	100.00

Table 6
Error matrix of 4-m-resolution image classification (%).

		Reference Image				
		Mango groves	Tropical secondary forests	Cultivated lands	Artificial surfaces	Water body
Evaluated Image	Mango groves	71.08	0.00	16.67	21.43	0.00
	Tropical secondary forests	1.20	95.00	26.67	0.00	0.00
	Cultivated lands	26.51	5.00	56.67	0.00	0.00
	Artificial surfaces	0.00	0.00	0.00	76.79	0.00
	Water body	0.00	0.00	0.00	1.79	100.00
	Others	1.20	0.00	0.00	0.00	0.00
	Total	100.00	100.00	100.00	100.00	100.00

Table 7
Error matrix of 8-m-resolution image classification (%).

		Reference Image				
		Mango groves	Tropical secondary forests	Cultivated lands	Artificial surfaces	Water body
Evaluated Image	Mango groves	72.29	0.00	23.33	51.79	0.00
	Tropical secondary forests	0.00	25.00	0.00	0.00	0.00
	Cultivated lands	27.71	75.00	76.67	0.00	0.00
	Artificial surfaces	0.00	0.00	0.00	46.43	0.00
	Water body	0.00	0.00	0.00	1.79	100.00
	Others	0.00	0.00	0.00	0.00	0.00
	Total	100.00	100.00	100.00	100.00	100.00

16.67% of cultivated lands were divided into mango groves. At the resolution of 8 m, 27.71% of mango groves were divided into cultivated lands and 23.33% of cultivated lands were divided into mango groves. At the resolutions of 1, 2, and 4 m, there was a phenomenon of mango grove leakage into tropical secondary forests, but the extent of leakage was small. At the resolution of 8 m, the probability of mango grove leakage into tropical secondary forests was 0, and the separation between mango groves and tropical secondary forests was the best. A comparative analysis of the extraction accuracy of artificial surfaces under the four resolutions shows that with the decrease in spatial resolution, the phenomenon of artificial surfaces being misclassified as mango groves becomes increasingly pronounced. When the spatial resolution is 1 m, 5.36% of artificial surfaces are misclassified as mango groves, whereas when the spatial resolution is 8 m, 51.79% of artificial surfaces are misclassified as mango groves. This is mainly because the green belt around residential buildings and on both sides of roads in the study area will form mixed pixels with the decrease in spatial resolution, and the mango groves will also form mixed pixels with the bare ground between rows and trees with the decrease in spatial resolution, and the two mixed pixels are difficult to distinguish in spectrum, thus reducing the extraction accuracy of mango groves. In general, under the four resolutions, the mixed separation of mango groves and cultivated lands is clear, and cultivated lands are the main type of land that reduced the extraction accuracy of mango groves. The mixing between tropical secondary forests and mango groves is limited, but with the decrease in spatial resolution, the mixing between artificial surfaces and mango groves will gradually become severe in terms of misclassification rate.

To visually compare the classification results under four spatial resolutions, the classification results of the research area under different resolutions are presented in Fig. 4. By comparing the classification results in Fig. 4, it can be found that owing to the planting of green vegetation near artificial surfaces such as buildings and roads, the phenomenon of artificial surfaces being misclassified as mango groves increases with the decrease in spatial resolution. The higher the spatial resolution, the higher the extraction accuracy of artificial surfaces. There is little difference in the spatial distribution range of mango groves at the spatial resolutions of 1 and 2 m. Cultivated land is the main factor that reduces the extraction accuracy of mango groves at the two resolutions, but the remote sensing images with both spatial resolutions can ensure a certain

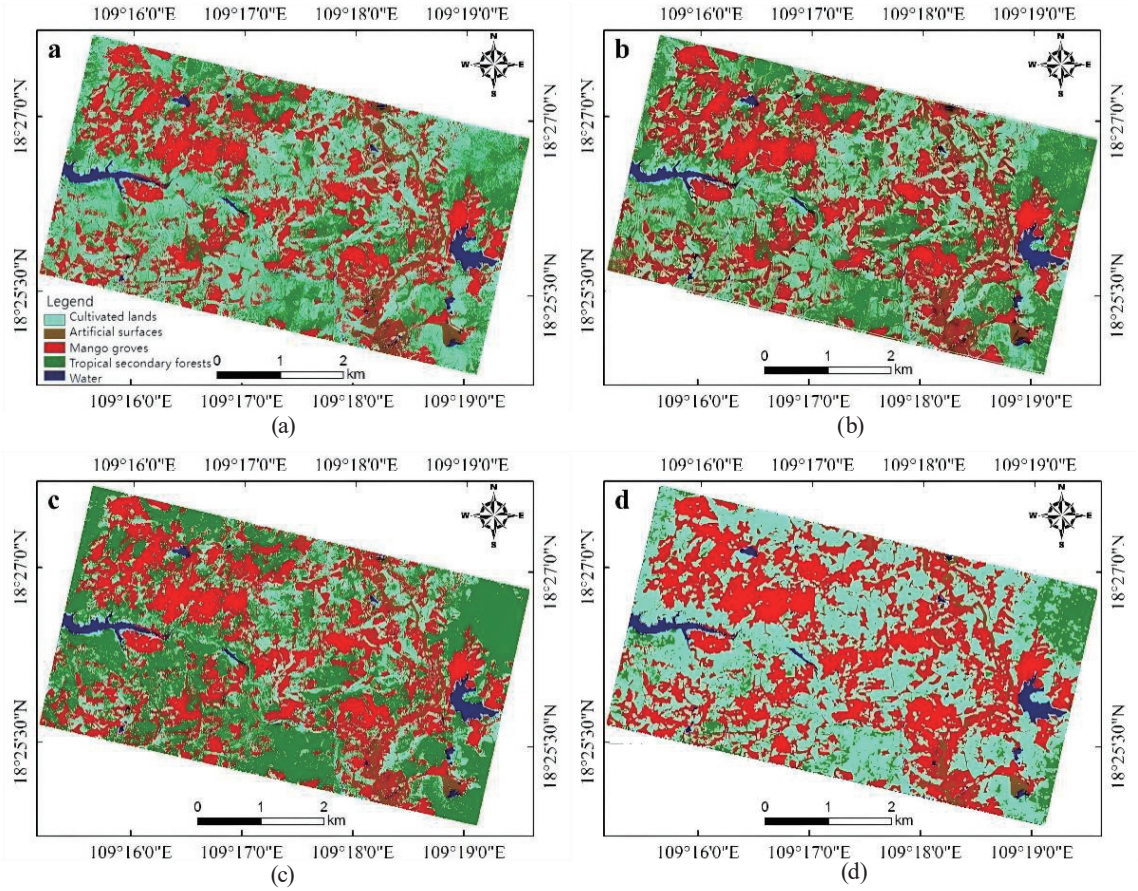

Fig. 4. (Color online) Classification maps of the study area at different resolutions: (a) 1-m-resolution image, (b) 2-m-resolution image, (c) 4-m-resolution image, and (d) 8-m-resolution image.

extraction accuracy of mango groves. At the resolutions of 4 and 8 m, the leakage and misclassification of mango groves were clear and the extraction accuracy of mango groves was reduced overall.

4. Discussion and Conclusions

In this study, considering the data processing efficiency and the characteristics of mango tree planting intervals of 3 to 4 m, the applicability of extracting the spatial distribution of mango groves from images with different spatial resolutions by using only the spectral information of images was demonstrated. In this study, with the 1-m-resolution GF-2 fusion image as the basic data, resampling images with the resolutions of 2, 4, and 8 m were obtained by the pixel clustering method, and SVM was used to classify remote sensing images with four resolutions. Finally, validation sample data were selected from the ground sampling data for the quantitative evaluation of classification results. The results showed that there was little difference in the spatial distribution range of mango groves at the resolutions of 1 and 2 m, but the mapping and

user accuracies of mango groves at the resolutions of 2 m were higher. At the 4 m resolution, the extraction accuracy of mango groves decreased, and cultivated land was the main factor to reduce the extraction accuracy of mango groves. At the resolution of 8 m, the mixing of mango groves and cultivated lands was more pronounced. Therefore, when only the spectral information of remote sensing image is used, the image with a resolution of 2 m is the best image extracted by the remote sensing of mango groves.

Through the error matrix analysis of remote sensing image classification results at different spatial resolutions, it can be seen that cultivated land is the main land class that reduces the extraction accuracy of mango groves when only the spectral information of the remote sensing image is used. Under the four resolutions, the mixing phenomenon of mango groves and cultivated lands becomes increasingly pronounced as spatial resolution decreases. With the decrease in spatial resolution, the probability of artificial surfaces being misclassified as the mango groves increases. Moreover, it would be valuable to systematically evaluate the performance of a broader range of models, including deep learning architectures, random forest, and the SVM method employed in this study. A comprehensive comparative analysis would elucidate their specific advantages and limitations, thereby informing the development of more robust and efficient protocols for operational monitoring.

References

1 G. Zhao, Q. Liu, and P. Peng: J. Agric. Sci. Technol. **24** (2022) 111. https://doi.org/10.13304/j.nykjdb.2021.0409
2 P. S. Roy, M. D. Behera, and S. K. Srivastav: Proc. National Academy of Sciences, India Section A: Physical Sciences **87** (2017) 465. https://doi.org/10.1007/s40010-017-0428-8
3 H. Ye, W. Huang, B. Cui, Y. Dong, S. Huang, and C. Ren: 2018 7th Int. Conf. Agro-geoinformatics (Agro-geoinformatics) (2018) 1. https://doi.org/10.1109/Agro-Geoinformatics.2018.8476135
4 W. J. Moses, S. G. Ackleson, J. W. Hair, C. A. Hostetler, and W. D. Miller: J. Geophys. Res. **121** (2016) 4194. https://doi.org/10.1002/2016JC011767
5 H. Xin, Z. Liang-Pei, and L. I. Ping-Xiang: J. Remote Sens. **02** (2007) 193. https://doi.org/10.11834/jrs.20070226
6 J. Hu, G. S. Xia, F. Hu, and L. Zhang: Remote Sens. **7** (2015) 14988. https://doi.org/10.3390/rs71114988
7 Y. Liu, Y. Zhong, and S. Z. L. Shi: ISPRS J. Photogramm. Remote Sens. **209** (2024) 296. https://doi.org/10.1016/j.isprsjprs.2024.01.013
8 Z. Xu and E. Y. Lam: J Opt Soc Am A Opt Image Sci. Vis. **27** (2010) 1638. https://doi.org/10.1364/JOSAA.27.001638
9 T. Feng, H. Ma, X. Cheng, and H. Zhang: J. Appl. Remote Sens. **12** (2018) 1. https://doi.org/10.1117/1.JRS.12.025006
10 D. Marceau and G. Hay: Canadian J. Remote Sens. **25** (1999) 357. https://doi.org/10.1080/07038992.1999.10874735
11 B. L. Markham and J. R. G. Townshend: Proc. Int. Symp. Remote Sensing of Environment **3** (1981).
12 G. M. Foody: Remote Sens. Environ. **114** (2010) 2271. https://doi.org/10.1016/j.rse.2010.05.003
13 X. Lin, X. Wang, Z. Tang, M. Li, R. Wu, and D. Huang: Remote Sens. Technol. Appl. **39** (2024) 315. https://doi.org/10.11873/j.issn.1004-0323.2024.2.0315
14 J. Chen: Jiangxi University of Science and Technology **02** (2023) 1. https://doi.org/10.27176/d.cnki.gnfyc.2023.000904
15 W. Xie, Y. Zhang, L. Wu, L. Song, H. Zhang, and Y. Zhang: Xiandai nongji **02** (2023) 68. https://doi.org/10.26435/j.cnki.hnjj.2023.02.023
16 R. Ducay and D. W. Messinger: J. Appl. Remote Sens. **17** (2023) 024504. https://doi.org/10.1117/1.JRS.17.024504
17 S. Anand and R. Sharma: Eng. Res. Express **6** (2024) 022201. https://doi.org/10.1088/2631-8695/ad3a34
18 W. Sun, B. Chen, and D. W. Messinger: Opt. Eng. **53** (2014) 013107. https://doi.org/10.1117/1.OE.53.1.013107
19 L. Bo, Z. Qing-He, W. Yan, and T. G. University: Remote Sens. Inf. **31** (2016) 97. https://doi.org/10.3969/j.issn.1000-3177.2016.02.018
20 J. Wang, C. Du, and T. Gao: MIDA **2024** (2024) 666. https://doi.org/10.1145/3662739.3673680

21 H. H. Kanwal, I. Ahmad, and M. S. Aziz: ICMLC **2022** (2022) 197. https://doi.org/10.1145/3529836.3529842
22 G. Mountrakis, J. Im, and C. Ogole: ISPRS J. Photogramm. Remote Sens. **66** (2011) 247. https://doi.org/10.1016/j.isprsjprs.2010.11.001
23 Y. Bazi and F. Melgani: IEEE Trans. Geosci. Remote Sens. **44** (2006) 3374. https://doi.org/10.1109/TGRS.2006.880628
24 M. Wang, Y. Wan, Z. Ye, and X. Lai: Inf. Sci. **402** (2017) 50. https://doi.org/10.1016/j.ins.2017.03.027
25 D. Zeng, D. Li, Y. Ke, Y. Wu, X. Li, and H. Gong: Remote Sens. Nat. Resour. **28** (2016) 12. https://doi.org/10.6046/gtzyyg.2016.03.03
26 R. Pouteau, J.-Y. Meyer, R. Taputuarai, and B. Stoll: Ecol. Inf. **9** (2012) 37. https://doi.org/10.1016/j.ecoinf.2012.03.003